IDENTIFICATION AND REDUCTION OF DISTURBANCE FACTORS IN THE ACOUSTIC PROCESS MONITORING OF THE PBF-LB FOR QUALITY ASSURANCE

Peter Gross[1], Italo Balestra[2], Cristiano De Boni[2], Alexander Fritz[2], Johannes Schötz[2], Yaxiong Ren[3], Tobias Melz[3], Holger Merschroth[1], Matthias Weigold[1]

[1] Institute of Production Management, Technology and Machine Tools (PTW), Technical University of Darmstadt, Darmstadt, Germany

[2] OmegaLambdaTec GmbH (OLT), Garching, Germany

[3] System Reliability, Adaptive Structures, and Machine Acoustics (SAM), Technical University of Darmstadt, Darmstadt, Germany

Abstract

Powder bed fusion with laser beam for metals (PBF-LB/M) is widely used to produce complex parts for lightweight applications. Although there have been many investigations to set up an in-situ process monitoring for the PBF-LB/M, cost-intensive quality assurance is essential. Acoustic process monitoring is a promising approach due to high data rates with small memory requirements with a simple implementation and the possibility to detect subsurface defects. However, disturbance factors during the acoustic measurements affect the quality of defect detection. In this paper, we present an approach to identify and minimize disturbance factors by varying the process boundary conditions such as the reflection behavior of the build chamber while monitoring single line experiments. Subsequently the impact of the build chamber reflection on the data quality is evaluated by a comparative analysis. This work shows that a careful consideration of the boundary conditions plays a crucial role to ensure reliable defect detection.

Introduction

Metal Additive Manufacturing (AM) has been used significantly more in various industries in recent years due to its potentials of producing highly complex parts. Compared to conventional manufacturing processes, the use of additive manufacturing can lead to cost savings, a reduction in material waste and greater design freedom [1]. During the PBF-LB/M process parts are build up layer by layer using a laser beam to melt metal powder to a dense part. Therefore, each layer consists of an appropriate scan path which is defined by the scan strategy and the part geometry. The scan path consists of multiple scan vectors which are lined up and stacked during the process to manufacture a part.

Despite its significant potential for the manufacturing industry, process instability and inconsistent part quality continue to pose major challenges to the widespread adoption of the technology [2]. A variety of defects can occur in AM parts that manifest themselves during the process or later in the finished part, resulting in rejects and therefore cost-intensive quality

assurance is required [3]. Rejects lead to waste of machining time and of material or the material must be recycled within an elaborate process. In both cases, resources are wasted, additional CO_2 is emitted and the economic feasibility of the process is reduced.

Such defect patterns can be divided into three groups: Microstructural defects, geometric defects and process events [3]. As the investigations are carried out based on single lines, this study analyzes the class of process events. This class includes events such as the balling effect, melt track breaks or contour elevations. (see Figure 1).

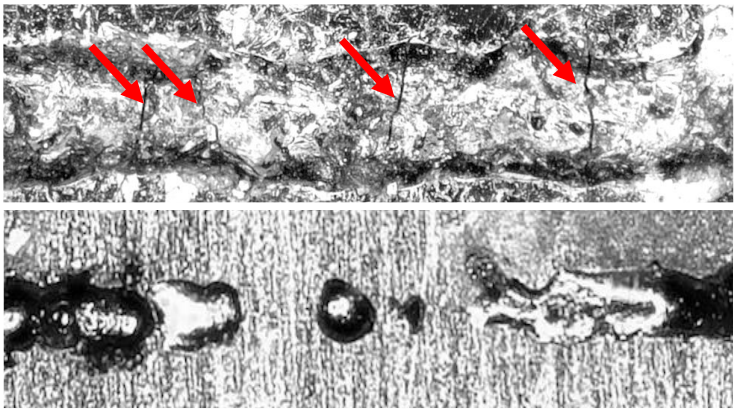

Figure 1: Melt track cracks, marked by red arrows (top); balling with lack of fusion (bottom)

Monitoring and the ability to detect such process events is essential, as these are often the cause of error patterns that occur in the finished part [3]. A continuous melt track with a stable geometry is therefore crucial in PBF-LB [4]. The resulting defects in the finished part can be pores, cracks or increased surface roughness as shown in Figure 2.

Figure 2: Defect patten in the final part; low density (top left) vs. high density parts (top right); surface roughness (bottom)

There are currently several approaches for detecting process events, most of them based on the use of optical process monitoring systems such as high-speed cameras, photodiodes,

pyrometers and optical tomography systems [5]. However, the formation of plume in the process, low sampling rates and often large amounts of data lead to distortions, low resolutions and long computational processing times. At this point, acoustic process monitoring approaches offer the possibility of obtaining much higher resolution data with a comparatively small memory capacity requirement and also avoiding distortions caused by process influences such as plume formation.

In recent years, various studies have demonstrated the potential for defect detection through acoustic process monitoring. For example, keyhole pores could be provoked by a specific sample design and classified by an support vector machine algorithm with an accuracy up to 97% [6]. The specific sample design also enables constant process parameters and thus keeps the controllable influencing factors as constant as possible. In addition, the potential for detecting subsurface defects using acoustic process monitoring was demonstrated. Therefore M. Seleznev *et al* (2022) detect cracks in the component during the manufacturing process with the help of structure-borne sound data collected with an acoustic emission AE-sensor [7]. Approaches for density prediction using acoustic process monitoring are also presented in other papers [8,9]. However, the controllable influencing factors such as laser power, scanning speed or hatching are often modified, which can lead to uncertainties in the correlation between the resulting acoustic signals and the underlying process parameters as well as the resulting defects.

In addition to the controllable influencing factors, there are also many uncontrollable influencing factors in acoustic process monitoring. One influencing factor is the reflection behavior of the build chamber. Many of the current PBF-LB systems have flat, smooth metallic surfaces on the walls of the build chamber. These sound hard surfaces reflect the sound wave with minimum damping and thus generate an echo in the build chamber. However, previous works on process monitoring using airborne sound have not taken this phenomenon into account.

Current approaches for acoustic process monitoring in PBF-LB often neglect the disturbances present within the build chamber. Environmental factors such as machine vibrations, airflow patterns, build chamber reflection and ambient noise can significantly impact signal clarity and interpretation [10]. Thus, there is a crucial need to develop robust methodologies for identifying and mitigating disturbances in the build chamber. Such efforts will not only improve the accuracy and reliability of acoustic monitoring but also enhance overall quality assurance in PBF-LB processes, thereby facilitating broader adoption of AM technologies in manufacturing industries.

The work presented below was carried out as part of the ML-S-LeAF project - “Development of machine learning algorithms on the basis of virtual sound data for lightweight construction for quality assurance in additive manufacturing” - which is funded by the BMWK.

Research methodology

A PBF-LB system from EOS GmbH was used for the investigations. This is the model M290 with a chamber volume of $250x250x300\ mm$ and a 400 W single-mode fiber laser with a wavelength of $1060\ nm$ and a focus diameter of $100\ \mu m$. Gas atomized stainless steel powder 316L is used for all experiments. The system is equipped with two 1/4" MM 302 measuring microphones from Microtech Gefell GmbH for the experiments (see Figure 3, Microphone 1 (M1), Microphone 2 (M2)).

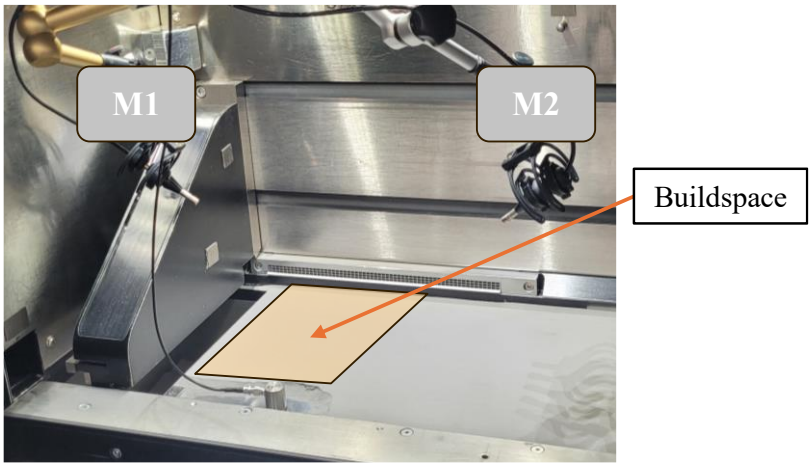

Figure 3: Experimental setup

These are free-field microphones with a frequency range of $5\ Hz\ to\ 100\ kHz$, a limit sound pressure level of $168\ dB$ and an operating temperature of $-25°C\ to\ 100°C$. The sound pressure is measured in Pa. The airborne sound data is recorded via a National Instruments measuring system with a sampling rate of $600\ kHz$. In addition, the machine data (x,y position of the laser, modulation of the laser) and the data from the Melt Pool Monitoring System (MPM system) from EOS GmbH are recorded via the same interface at a sampling rate of $60\ kHz$ (see Figure 4).

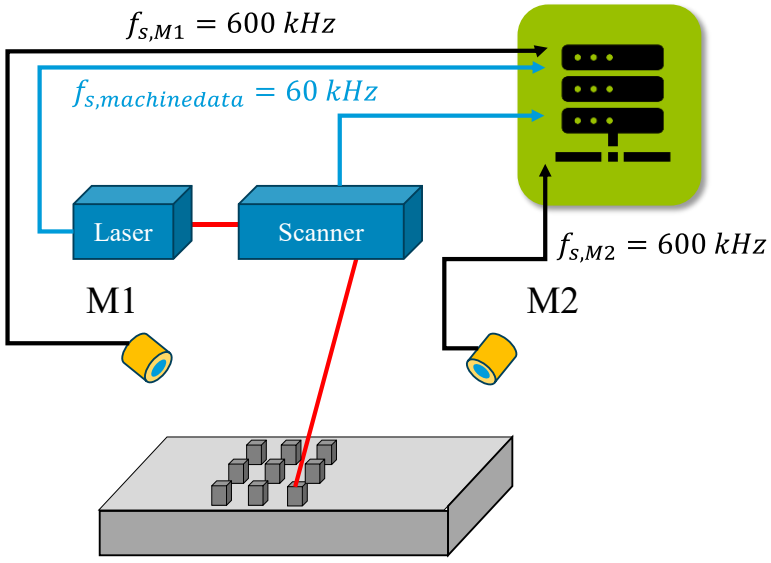

Figure 4: Overview of data acquisition

The machine data is used as a trigger signal to segment and label the sound data according to the process. Thereby, the one-dimensional sound data can be localized in two-dimensional space and each data point can be assigned a position on the building platform and thus individual scan vectors. In pre-processing, the position-dependent time offset of the airborne data due to the speed of sound propagation in argon at room temperature of approx. $323\ \frac{m}{s}$ [11] is taken into account and corrected by position compensation.

Single lines are produced as a test series. This reduces the complexity of the process and enables a clear assignment of sound data and scan vectors. In addition, spaceholders (area exposures with a laser power of $0\ W$) are produced after each single line in order to avoid inducing any process-related excitation during these intermediate times and thus to be able to isolate the sound data of each single line (see Figure 5). The figure shows two spectrograms that were generated using Short Time Fourier Transformation (STFT) ($nperseg = 512$, $overlap = 256$). After the end of the process, increased amplitudes are still detected over a broad frequency band, which slowly flatten out over time. This phenomenon is from now on referred to as a tail, whereby it is hypothesized that this is partly due to process noise reflected from the building chamber, which is referred to below as echo. The left part of the figure shows the spectrogram of two single lines produced directly after each other. It is assumed that the signal of the second line is strongly influenced by the superimposition of the tail of the previous scanned vector. To minimize this influence, the above-mentioned spaceholders are produced between all scan vectors. The resulting spectrogram of such an isolated line can be seen in the right part of Figure 5.

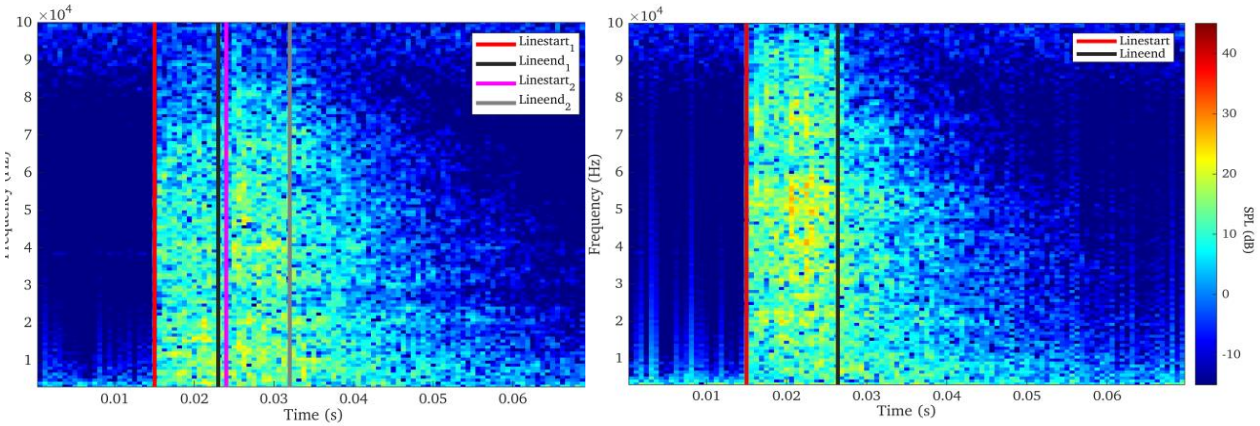

Figure 5: Spectrogram of two consecutive scan vectors (left) and a single scan vector (right)

The aim of this work is to minimize the influencing factors on the recorded signal to be able to assign the recorded data to the process sufficiently. Under the assumption that process noise causes an echo in the process chamber, it can be assumed that the process noise at the beginning of each scan vector influences the data recorded in the following. To investigate and minimize this influence, the build chamber is lined up with damping material (see Figure 6).

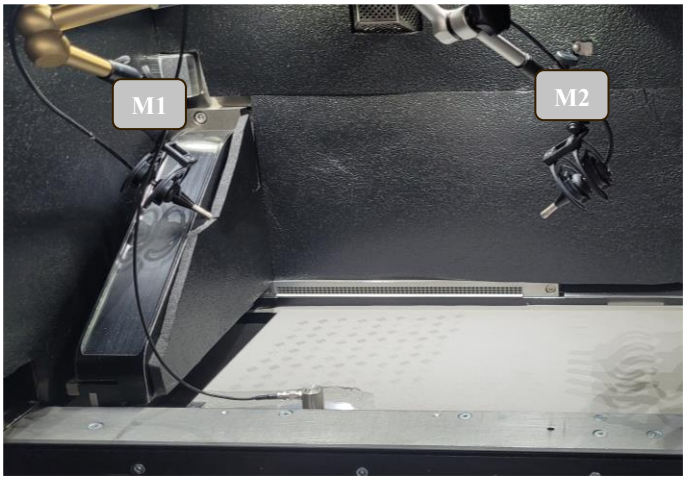

Figure 6: Build camber with microphones and damping material

100 individual lines with and without damping material were produced in each quadrant of the build plate. In addition, 50 individual lines with and 50 without damping material were produced, distributed across the entire build plate. All lines are produced on square base bodies with an edge length of 10 mm, which are built up in a previous job. This allows the target layer height of 60 μm to be set reliably and reproducibly. The base bodies have three grooves orthogonal to the production direction of the lines (see Figure 7).

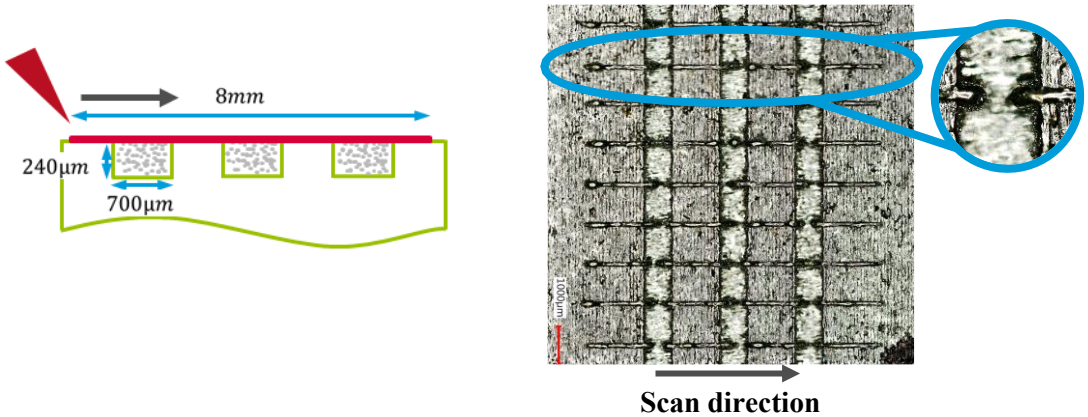

Figure 7: Sketch of the experimental design (left). Microscopic picture of one final specimen with 9 lines (right)

These grooves represent spontaneous variations in layer height during the process and induce anomalies in the single lines at predefined points which are similar to regular melt track breaks Assuming that the signal of regular, stochastically distributed process events is influenced by the echo to the same extent as the signal of the specifically induced anomalies, these anomalies are used as a quality criterion for the quantitative evaluation of the influence of the echo. An analysis of the recorded data is presented below, which provides information on the qualitative and quantitative differences in acoustic process monitoring caused by the use of damping material.

Results

After gathering the data, a first indication of the damping material's impact on the process camber behavior was observed. Looking at the spectrograms for lines printed with and without damping material, it can be obtained that there is a visual difference between these spectrograms. This difference is most obvious in the period after the end of production of the lines (see Figure 8).

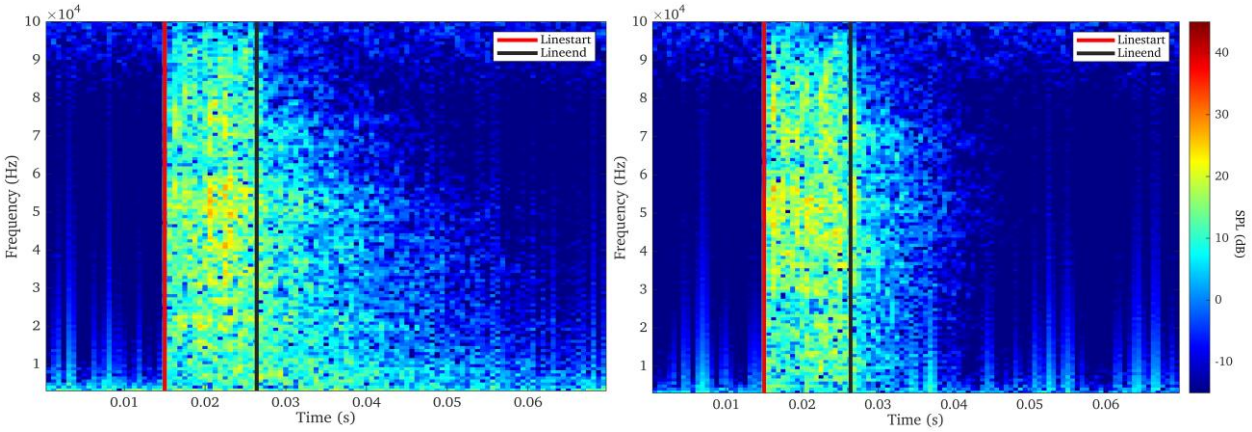

Figure 8: Spectrograms for lines without (left) and with damping material (right)

At this point, the assumption that the tail after the single line in the audio signals is influenced by the damping material in the build chamber and that it is mainly the sound waves reflected from the process chamber walls is confirmed. To be able to make a statement as to whether and to what extent the recorded sound data of a single line is influenced by its own echo, only the data recorded between the start and end of the line is evaluated below.

A significance test and a Principal Component Analysis (PCA) were carried out in order to make a basic statement as to whether the sound data of a single line is influenced by its own echo. To increase the number of samples for the significance test, the data of each line was divided into five time series of equal length. The sound pressure level was then calculated for each of these time series and the generated data was used for the significance test. For the PCA, the STFT spectrograms ($nperseg = 256$, $overlap = 128$) of each line were analyzed. The results of these investigations can be seen in Figure 9

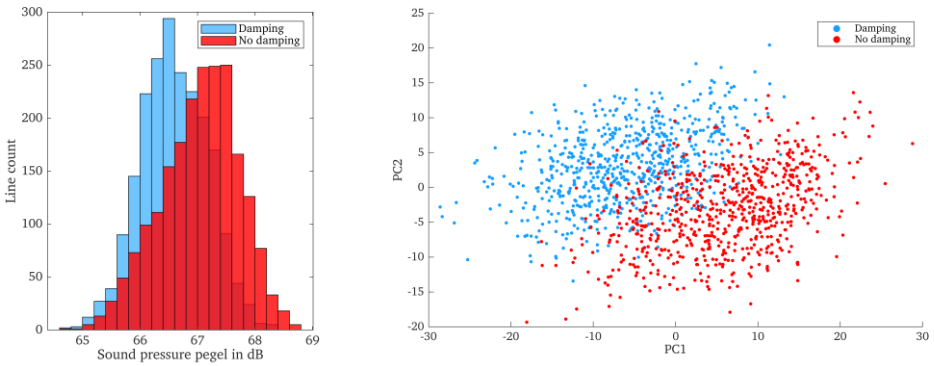

Figure 9: Results of the significance test (left), results for the PCA (right)

Results show that there are two distributions. As part of the significance test, a P value of $P < 0.001x^{10-23}$ with a confidence interval of $0.39 - 0.49\ dB$ can be shown with a significance level of $\alpha = 0.001$. The two data sets therefore differ significantly. The PCA plot also shows that the two data sets differ in two populations based on the first two components which represent about 38% of the variance in the data. This leads to the conclusion that the data differ qualitatively.

To quantify the qualitative differences shown above, two approaches are pursued based on of the data from one quadrant. On the one hand, an Extra Tree Regressor machine learning classifier is built. On the other hand, a data point-based classification is developed using the wavelet transform and various methods of time series processing. The pre-processing of the data for the machine learning model takes place in two steps. In the first step, the time series data of each line is transformed into spectrograms using STFT (same as for PCA) and is then divided into seven segments (see Figure 10).

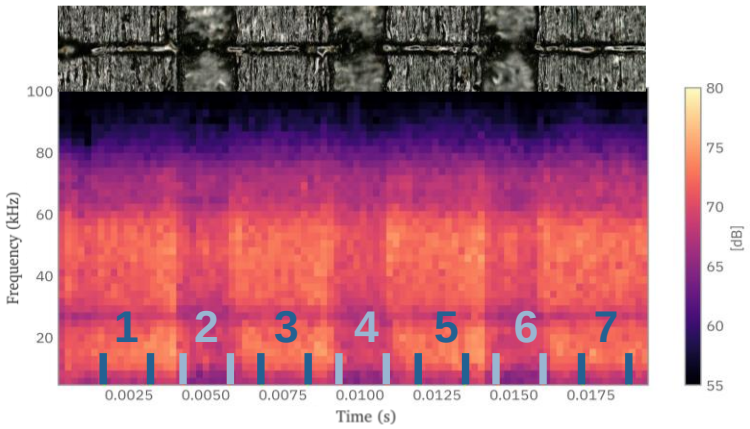

Figure 10: Segmentation of the STFT spectrograms with an example of a stacked spectrogram of 100 lines

In the figure, the stacked spectrogram of 100 lines was used as an example to illustrate the segmentation. For the evaluation, the segmentation is based on the individual spectrograms. Segments 1,3,5 and 7 correspond to good, defect free parts of the single line. Segments 2,4 and 6 correspond to defective areas. A two-dimensional spectrum is derived for each segment by averaging the amplitudes over time. These spectra are used as good and defective labeled data for modeling the classifier. A training/test data split of 80/20 is used. Figure 11 shows the results for both data sets in the form of confusion matrices.

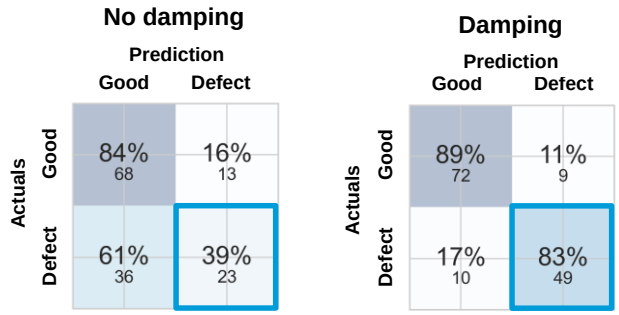

Figure 11: Confusion matrices for the results without damping material (left) and with damping material (right)

There is an improvement in the true-negative rate from 39% without damping material to 83% with damping material. The true-negative rate represents the segments correctly identified as defects and is therefore referred to as accuracy below, when only the defective class is considered. The results thus show that by reducing the echo in the process chamber, defect detection can be improved by a factor of 2,1 using acoustic process monitoring.

As the spectra are also provided with the labels 1-7, the data can also be evaluated with regard to the detection of the individual defective segments 2,4 and 6. The results can be seen in Figure 12 on the left.

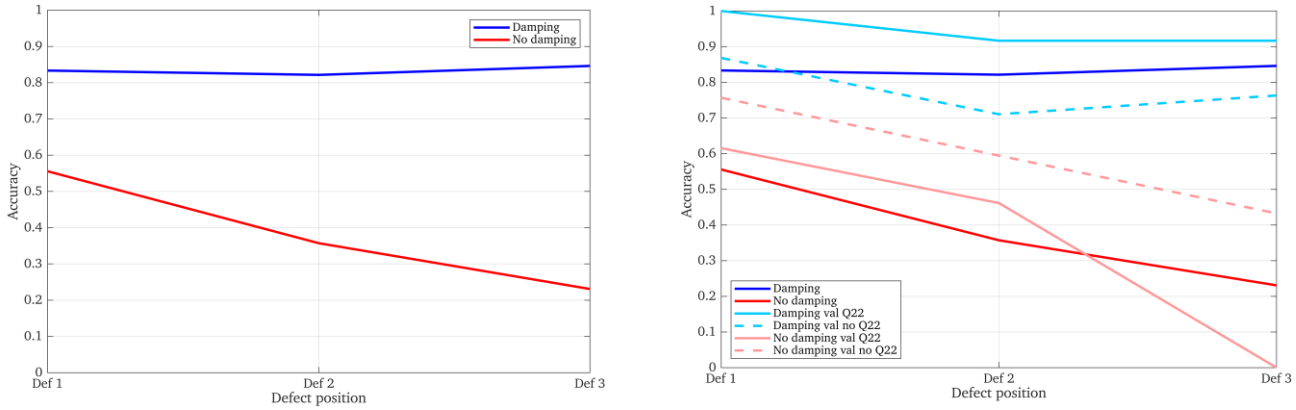

Figure 12: Accuracy results along the defect position for train/test data (left) and validation data (right)

The accuracy as a function of the position of the defective segments for the two data sets can be seen. Without the use of damping material, the accuracy over the position decreases (red graph), whereas the accuracy remains constant with the use of damping material (blue graph). This result suggests that the hypothesis "*the process noise at the beginning of each scan vector influences the data recorded in the following*" is correct. The right-hand side of Figure 12 also shows the results of the validation data set in light blue and light red. A distinction is made between data that was recorded in the same quadrant as the training data and data that was recorded in one of the other quadrants. It is clear to see that the performance of the models on the data of a separately produced build job is comparably good and shows the same trends. In this case, the deviations in accuracy are mainly due to stochastic deviation of comparatively small data sets.

As part of the second approach, the time series data is transformed into the frequency-time domain using wavelet transformation. There, the amplitudes are summed up and averaged in 10 kHz steps for each frequency band. The resulting two-dimensional signal is then globally normalized, derived and applied with a moving mean over the last 500 data points before the data of the individual frequency bands are merged again. The processed signal can be seen in light blue in Figure 13.

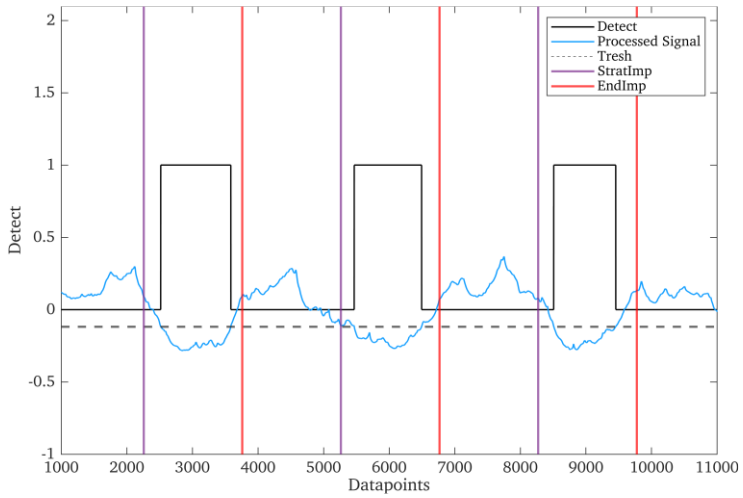

Figure 13: Reduction of the processed signal into a binary signal

The start (purple line) and endpoint (red line) of the grooves directly indicate the start end endpoints of an imperfect area in the line. The processed signal is reduced to a binary signal using a threshold (dashed line), whereby falling below the threshold represents a defect detection. The threshold was developed globally on the data set and optimized regarding the ratio between true negatives and true positives. Classification is performed for each data point of each single line. The resulting binary signals are then summed up and the result can be seen in Figure 14.

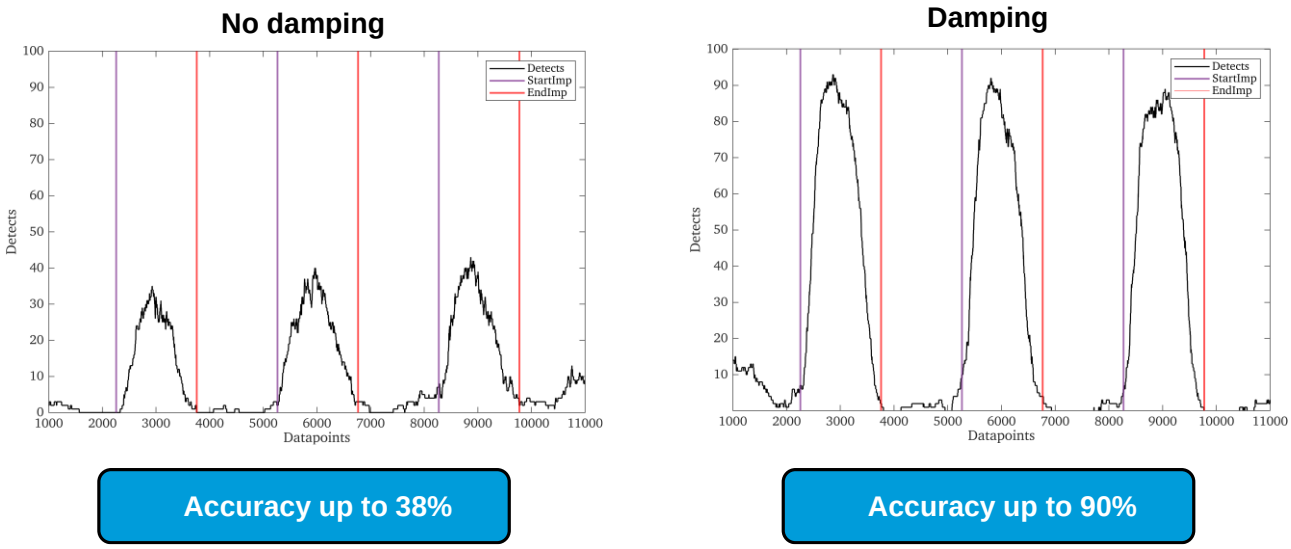

Figure 14: Results of the second approach without damping material (left) and with damping material (right)

The detected defects are plotted along the number of data points for both data sets. The start and end points of the grooves are also marked. The detected defects within a groove area are to be interpreted as correctly detected defects and thus formally correspond to the true negatives from the previous approach. The derived values are also listed under the term Accuracy. Like the previous approach, an improvement by the factor of 2,4 in accuracy from up to 38% without damping material to up to 90% with damping material is demonstrated.

Summary and outlook

In this work, the example of the build chamber reflection was used to show that a careful consideration of the boundary conditions plays a crucial role to ensure reliable defect detection with acoustic process monitoring approaches. For this purpose, two free-field microphones were sampled at a sampling rate of 600 kHz to detect sound emissions during the production process. Single lines were produced on base bodies with grooves. The grooves were used to introduce anomalies into the single lines, which were then used to qualitatively and quantitatively evaluate the influence of the build chamber reflection. Using significance tests and principal component analyses, it was possible to show qualitatively that the reflections of the process sound have a significant influence on the recorded signals and thus their quality. The influence was then quantified using two approaches. Both approaches showed comparable results and an increase in the defect detection rate by a factor of 2 by using damping material in the chamber. It was also shown that the signal is already influenced within a scan vector by the reflection of the own process excitation.

Future research will focus on expanding the evaluation methodology to account for additional influencing factors acoustic process monitoring. For this purpose, influence factors such as the inert gas flow, the position and orientation of the microphones and the scan direction of the lines are specifically varied. After the comprehensive evaluation of the influencing factors, the monitoring approach is extended from the consideration of single lines to the consideration of exposed surfaces and later to built-up volumes. In addition, the potential to fuse the airborne sound data from the microphones with the structure-borne sound data from acoustic emission sensors will be investigated to improve the quality of this process monitoring approach.

Further research in this field will enable process monitoring as a quality assurance tool, thereby replacing cost-intensive, downstream quality assurance with process-parallel quality assessment.

Acknowledgements

This research and development project is funded by the Federal Ministry for Economics and Climate Action (BMWK) within the “Technologietransfer-Programm Leichtbau” Program (funding number 03LB5006) and implemented by the Project Management Agency Jülich (PTJ). The authors are responsible for the content of this publication.

References

[1] C. Chua, Y. Liu, R. J. Williams, C. K. Chua und S. L. Sing, "In-process and post-process strategies for part quality assessment in metal powder bed fusion: A review", *Journal of Manufacturing Systems*, ed. 73, p. 75–105, 2024, doi: 10.1016/j.jmsy.2024.01.004.

[2] B. Zhang, Y. Li und Q. Bai, "Defect Formation Mechanisms in Selective Laser Melting: A Review" (En;en), *Chin. J. Mech. Eng.*, ed. 30, No. 3, p. 515–527, 2017, doi: 10.1007/s10033-017-0121-5.

[3] VEREIN DEUTSCHER INGENIEURE, "VDI 3405 Part 2.8 Additive manufacturing processes Powder bed fusion of metal with laser beam (PBF-LB/M) Defect catalogue – Defect images during laser beam melting ", 2022.

[4] D. Kouprianoff, N. Luwes, E. Newby, I. Yadroitsava und I. Yadroitsev, "On-line monitoring of laser powder bed fusion by acoustic emission: Acoustic emission for inspection of single tracks under different powder layer thickness" in *2017 Pattern Recognition Association of South Africa and Robotics and Mechatronics (PRASA-RobMech)*, Bloemfontein, South Africa, 2017, p. 203–207, doi: 10.1109/RoboMech.2017.8261148.

[5] M. Grasso, A. Remani, A. Dickins, B. M. Colosimo und R. K. Leach, "In-situ measurement and monitoring methods for metal powder bed fusion: an updated review", *Meas. Sci. Technol.*, ed. 32, No. 11, p. 112001, 2021, doi: 10.1088/1361-6501/ac0b6b.

[6] J. R. Tempelman *et al.,* "Detection of keyhole pore formations in laser powder-bed fusion using acoustic process monitoring measurements", *Additive Manufacturing*, ed. 55, No. 23, p. 102735, 2022, doi: 10.1016/j.addma.2022.102735.

[7] M. Seleznev *et al.,* "In situ detection of cracks during laser powder bed fusion using acoustic emission monitoring", *Additive Manufacturing Letters*, ed. 3, p. 100099, 2022, doi: 10.1016/j.addlet.2022.100099.

[8] N. Eschner, L. Weiser, B. Häfner und G. Lanza, "Classification of specimen density in Laser Powder Bed Fusion (L-PBF) using in-process structure-borne acoustic process emissions", *Additive Manufacturing*, ed. 34, Pg. 101324, 2020, doi: 10.1016/j.addma.2020.101324.

[9] R. Drissi-Daoudi, G. Masinelli, C. de Formanoir, K. Wasmer, J. Jhabvala und R. E. Logé, "Acoustic emission for the prediction of processing regimes in Laser Powder Bed Fusion, and the generation of processing maps", *Additive Manufacturing*, ed. 67, No. 23, p. 103484, 2023, doi: 10.1016/j.addma.2023.103484.

[10] J. Shao und Y. Yan, "Review of techniques for on-line monitoring and inspection of laser welding", *J. Phys.: Conf. Ser.*, ed. 15, p. 101–107, 2005, doi: 10.1088/1742-6596/15/1/017.

[11] W. M. Haynes, D. R. Lide und T. J. Bruno, *CRC Handbook of Chemistry and Physics*. CRC Press, 2016.